migration of its Zr-bound methylene group. The increased ring strain that would be introduced by such a 1,2-methylene shift apparently provides a sufficient activation barrier to preclude its occurrence. Molecular orbital calculations on **1** and **2** will be undertaken to evaluate the orbital character of the LUMO in these complexes. Their outcome may provide further insight into the role of the respective η^2-iminoacyl carbon centers in the overall reductive coupling process.

Acknowledgment. Support for this research was provided by the donors of the Petroleum Research Fund, administered by the American Chemical Society. J.L.P. further expresses his appreciation to Dr. P. Fagan and Professors W. R. Moore and A. Stolzenberg for helpful suggestions. Computer time for the X-ray structural analyses was provided by the West Virginia Network for Educational Telecomputing.

Supplementary Material Available: Tables of thermal parameters, pertinent least-squares planes for **3** and **5**, and the atomic coordinates for the hydrogen atoms of **3** (12 pages); listings of observed and calculated structure factors for **3** and **5** (19 pages). Ordering information is given on any current masthead page.

In-Plane Olefin Coordination and Unusually Small Substituent Dependency of Stability in (η^3-Allyl)(pentafluorophenyl)(olefin)-platinum(II) Complexes

Hideo Kurosawa,* Kunio Miki,† Nobutami Kasai,* and Isao Ikeda

Department of Applied Chemistry, Faculty of Engineering, Osaka University, Suita, Osaka 565, Japan

Received September 7, 1990

The crystal structure of the styrene complex Pt(η^3-CH_2CMeCH_2)(CH_2=CHC_6H_5)(C_6F_5) (**2a**) was determined. Crystal data: $C_{18}H_{15}F_5Pt$, fw = 521.40, triclinic, space group $P\bar{1}$, a = 6.292 (2) Å, b = 11.874 (4) Å, c = 12.736 (4) Å, α = 117.39 (2)°, β = 82.07 (3)°, γ = 97.50 (4)°, V = 834.3 (5) Å^3, Z = 2, D_c = 2.075 g cm^{-3}, R = 0.074 for 3410 reflections ($|F_o| > 3\sigma(|F_o|)$). The structure thus determined revealed the C=C bond of styrene oriented parallel to the coordination plane (the angle between the C=C axis and the coordination plane is 10.2°). When dissolved in $CDCl_3$, **2a** takes two isomeric forms. The ^{1}H NMR NOE experiments indicated that the configuration of the major isomer in solution is similar to that in the solid state. The minor isomer corresponds to a diastereomer of the major isomer, where both isomers contain the C=C bond lying almost in the coordination plane. The measurements of the epimerization rate of **2a** in the absence and presence of free styrene suggested that the interconversion between the two isomers is an intramolecular process without invoking Pt–styrene bond dissociation. Substituted styrene complexes Pt(η^3-CH_2CMeCH_2)(CH_2=CHC_6H_4Y)(C_6F_5) (**2b–f**) (Y = *m*-NO_2, *p*-Cl, *p*-Me, *p*-OMe, *o*-Me) were generated by ligand exchange between **2a** and appropriate olefin. Relative olefin coordination ability was determined by ^{1}H NMR analysis of an equilibrium mixture containing **2a**, a substituted styrene complex, **2b–f**, and the appropriate olefins to show the stability trend unusually weakly dependent on the electronic property of the substituent Y (Hammett ρ = −0.38). The nature of the Pt–olefin bond in **2** has been discussed in terms of these stability and structural trends.

Olefin complexes of transition metals simultaneously containing η^3-allyl ligands have received increasing attention from both coordination[1] and synthetic[2] chemical points of view. The studies on the cationic olefin complexes of the type [Pt(η^3-CH_2CMeCH_2)(olefin)(PPh_3)]$^+$ (**1**)

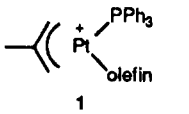

1

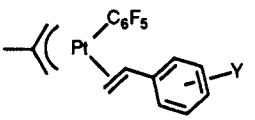

2a, Y = H
b, Y = *m*-NO_2
c, Y = *p*-Cl
d, Y = *p*-Me
e, Y = *p*-OMe
f, Y = *o*-Me

have revealed[1b] that these are somewhat unique in terms of the nature of metal–olefin bond when compared to the classic, more ordinary olefin complexes of Pt(II) such as Zeise's salt. That is, the former class complexes contain the C=C bond oriented parallel to the coordination plane (in-plane geometry)[1b,c,e] if the steric effect is not significant, in contrast to that oriented perpendicular (upright geometry) in the latter class.[3] This difference was brought about primarily by the different steric requirement around

† Present address: Research Laboratory of Resources Utilization, Tokyo Institute of Technology, Nagatsuda, Yokohama 227, Japan.

(1) (a) Grassi, M.; Meille, S. V.; Musco, A.; Pontellini, R.; Sironi, A. *J. Chem. Soc., Dalton Trans.* **1990**, 251–255. (b) Miki, K.; Yamatoya, K.; Kasai, N.; Kurosawa, H.; Urabe, A.; Emoto, M.; Tatsumi, K.; Nakamura, A. *J. Am. Chem. Soc.* **1988**, *110*, 3191–3198. (c) Musco, A.; Pontellini, R.; Grassi, M.; Sironi, A.; Meille, S. V.; Ruegger, H.; Ammann, C.; Pregosin, P. S. *Organometallics* **1988**, *7*, 2130–2137. (d) Ciajolo, R.; Jama, M. A.; Tuzi, A.; Vitagliano, A. *J. Organomet. Chem.* **1985**, *295*, 233–238. (e) Miki, K.; Kai, Y.; Kasai, N.; Kurosawa, H. *J. Am. Chem. Soc.* **1983**, *105*, 2482–2483. (f) Kurosawa, H.; Asada, N. *Organometallics* **1983**, *2*, 251–257. (g) Kurosawa, H.; Asada, N. *J. Organomet. Chem.* **1981**, *217*, 259–266.

(2) (a) Kurosawa, H.; Ogoshi, S.; Kawasaki, Y.; Murai, S.; Miyoshi, M.; Ikeda, I. *J. Am. Chem. Soc.* **1990**, *112*, 2813–2814. (b) Negishi, E.; Iyer, S.; Rousset, C. J. *Tetrahedron Lett.* **1989**, *30*, 291–294. (c) Oppolzer, W.; Bedoya-Zurita, M.; Switzer, C. Y. *Ibid.* **1988**, *29*, 6433–6436. (d) Kurosawa, H.; Emoto, M.; Ohnishi, H.; Miki, K.; Kasai, N.; Tatsumi, K.; Nakamura, A. *J. Am. Chem. Soc.* **1987**, *109*, 6333–6340. (e) Goliaszewski, A.; Schwartz, J. *Tetrahedron* **1985**, *41*, 5779–5789 and references therein. (f) Hosokawa, T.; Uno, T.; Inui, S.; Murahashi, S. *J. Am. Chem. Soc.* **1981**, *103*, 2318–2323.

(3) Ittel, S.; Ibers, J. A. *Adv. Organomet. Chem.* **1976**, *14*, 33.

0276-7333/91/2310-1607$02.50/0 © 1991 American Chemical Society

Table I. ^{1}H NMR Spectral Data for (η^3-Allyl)platinum Complexes[a]

complex	δ 1	2	3	4	5	6	7	Me
2a-maj	3.91[d] (J_H = 13.5, J_{Pt} = 54)	3.68[d] (J_H = 9, J_{Pt} = 54)	5.96[dd] (J_{Pt} = 61)	2.62[s] (J_{Pt} = 61)	3.78[br]	4.03[d] (J_H = 3)	3.08[s] (J_{Pt} = 40)	1.41[s] (J_{Pt} = 56)
2a-min	4.05[d] (J_H = 13.5, J_{Pt} = 52)	3.77[d] (J_H = 9)	5.31[dd] (J_{Pt} = 56)	2.54[s] (J_{Pt} = 64)	3.81[br]	4.33[br]	2.13[s] (J_{Pt} = 30)	1.92[s] (J_{Pt} = 60)
2b-maj	4.05[d] (J_H = 13, J_{Pt} = 57)	3.72[d] (J_H = 9, J_{Pt} = 54)	5.74[dd] (J_{Pt} = 57)	2.74[s] (J_{Pt} = 60)	3.89[br]	4.18[d] (J_H = 3)	3.11[s] (J_{Pt} = 40)	1.56[s] (J_{Pt} = 57)
2b-min	*b*	*b*	5.16[dd] (J_H = 9.5, 13, J_{Pt} = 59)	2.54[s] (J_{Pt} = 61)	*b*	4.49[d] (J_H = 3)	2.32[s] (J_{Pt} = 32)	1.99[s] (J_{Pt} = 60)
2f-maj[c]	3.88[d] (J_H = 12.5, J_{Pt} = 54)	3.75[d] (J_H = 10, J_{Pt} = 56)	6.11[dd] (J_{Pt} = 54)	2.63[s] (J_{Pt} = 63)	3.80[br]	4.07[d] (J_H = 3)	2.97[s] (J_{Pt} = 39)	1.49[s] (J_{Pt} = 54)
2f-min[d]	4.08[d] (J_H = 13, J_{Pt} = 54)	3.92[d] (J_H = 9)	5.58[dd] (J_{Pt} = 56)	*b*	3.78[br]	4.33[d] (J_H = 3)	2.19[s] (J_{Pt} = 31)	1.92[s] (J_{Pt} = 60)

[a] In $CDCl_3$ at 25 °C. δ in ppm; *J* in Hz. For proton numbering scheme, see text (3 and 4). Isomer ratios are 2.7/1 (**2a**), 2.0/1 (**2b**), and 2.2/1 (**2f**). [b] Overlapped with other resonances. [c] δ(*o*-Me) = 2.55[s]. [d] δ(*o*-Me) = 2.44[s].

the coordinated olefin between the two classes of complexes; there exists more room for the in-plane olefin in **1**. In terms of the electronic factor, the in-plane geometry in **1** was suggested[1b] to be only slightly more favored than the upright one, this trend being traced to a slightly larger π back-bonding in the former geometry. In fact, the π-back-bonding interaction in **1** is not very important, and the metal atom in **1** was as electrophilic in nature toward the coordinated olefin ligand[1f,g] as that in the ordinary complexes, *trans*-$PtCl_2$(olefin)(py).[4]

The larger π-back-bonding interaction is expected if some electron-donating ligands, such as hydrocarbyl ligands, are attached to the η^3-allylmetal moiety. This interaction was suggested to be indeed significant in complexes of the type Pd(η^3-allyl)(olefin)(Ar), both in the ground state and, in particular, in the transition state of the η^3-allyl–aryl coupling on Pd.[2d] These palladium complexes, however, were not sufficiently stable to allow a detailed structure and stability analysis. As an isolable model for this type of species, we prepared a platinum analogue, Pt(η^3-CH_2CMeCH_2)(CH_2=CHC_6H_5)(C_6F_5) (**2a**).[2d]

In order to gain more insight into the nature of the metal–olefin bond in complexes containing the η^3-allyl ligand, we undertook synthetic, stability, and structural studies of neutral analogues Pt(η^3-CH_2CMeCH_2)(CH_2=CHC_6H_4Y)(C_6F_5) (**2**).[5] Here we wish to report the structure determination of these complexes both in the solid state and in solution, which provided another example of an in-plane olefin coordination complex. These studies, together with solution stability trends, also show the novel Pt–olefin bonding nature as compared with that in **1** and other known Pt(II)–olefin complexes.

Results and Discussion

Formation of Pt(η^3-CH_2CMeCH_2)(CH_2=CHC_6H_4Y)(C_6F_5) (2). Neutral olefin complexes of Pt(II) containing the η^3-methallyl and perfluorophenyl groups **2a**, **2b**, and **2f** were synthesized by the reaction of C_6F_5Li with a mixture of dimeric η^3-methallylplatinum chloride and the olefin. The latter mixture was previously shown[1f] to be in equilibrium in solution with a monomeric olefin complex, Pt(η^3-CH_2CMeCH_2)(olefin)Cl. Once this monomer is arylated as in **2**, dissociation of the olefin ligand does not take place to an extent detectable by NMR spectroscopy. ^{1}H NMR spectral data for **2a**, **2b**, and **2f** are shown in Table I. The substituted styrene complexes **2b–f** were also generated in solutions by quite a slow ligand exchange between **2a** and the appropriate olefin and characterized by ^{1}H NMR spectra. The very slow ligand exchange in **2**, as discussed later, is in sharp contrast to the observation that the corresponding ligand exchange in **1** occurred almost instantaneously under the same conditions.[1b]

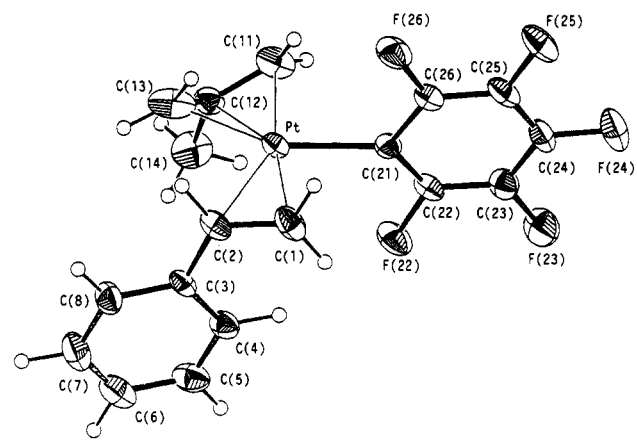

Figure 1. ORTEP drawing[16] of the molecular structure of Pt(η^3-CH_2CMeCH_2)(C_6F_5)(CH_2=$CHPh$) (**2a**) along with atomic numbering system. Non-hydrogen atoms are presented as thermal ellipsoids at 30% probability levels, whereas hydrogen atoms are drawn as spheres with B = 1.0 Å^2.

It was previously reported[2d] that the palladium analogues Pd(η^3-allyl)(olefin)(Ar) are very prone to undergo the reductive elimination to give the allylbenzene derivatives at below 0 °C. On the other hand, we have now found that compounds **2** were quite inert with respect to the reductive elimination when kept even at 70 °C for more than 5 h. A slow decomposition did occur under these conditions, but the only products that we could characterize included styrene and isobutene.

X-ray Crystal Structure Determination of Pt(η^3-CH_2CMeCH_2)(CH_2=CHC_6H_5)(C_6F_5) (2a). The structure of **2a** was determined by X-ray crystallography. The molecular structure is shown in Figure 1, and the relevant bond lengths and angles are in Table II. The complex is approximated as essentially a square-planar structure; the platinum atom, the ipso carbon atom C(21) of C_6F_5, the center of the C=C double bond (CET), and the center of gravity of the allyl triangle (CAL) make an average plane with maximum deviation being 0.04 Å.

It seems of interest to note that the C=C bond in **2a** makes an angle of 10.2° with the coordination plane defined by Pt, CAL, and C(21). This feature is the same as that in the cationic complex **1** (olefin = CH_2=CHC_6H_5).[1b] However, one of the Pt–C(olefin) bond lengths in **2a** (Pt–C(2) = 2.23 (2) Å) is considerably shorter than that

(4) Kurosawa, H.; Urabe, A.; Emoto, M. *J. Chem. Soc., Dalton Trans.* **1986**, 891–893.
(5) Preliminary communication: (a) Kurosawa, H.; Ikeda, I. *Chem. Lett.* **1989**, 1989–1992. (b) Kurosawa, H.; Ohnishi, H.; Miki, K.; Kasai, N.; Tatsumi, K.; Nakamura, A. *Ibid.* **1987**, 1623–1626.

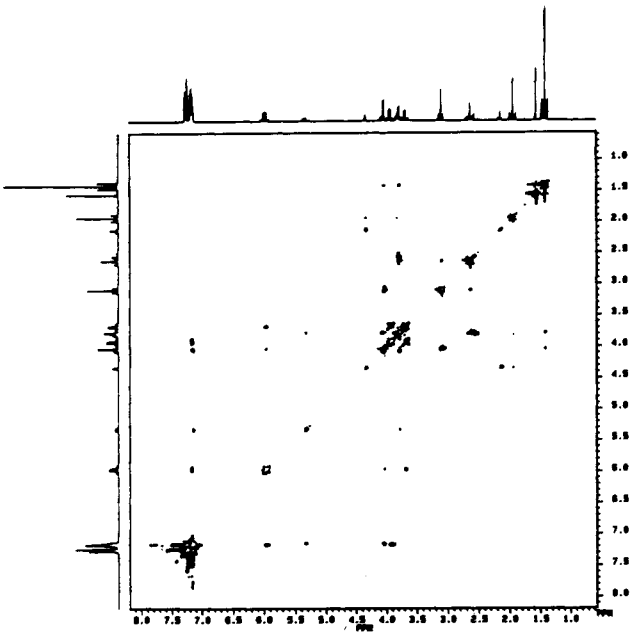

Figure 2. 600-MHz phase-sensitive NOESY spectrum of **2a**. Negative peaks appeared only at the diagonal positions. Mixing time was 4 s with 90° excitation and mixing pulses used.

in the cationic complex (2.30 (1) Å),[1b] while the other Pt–C(olefin) bond is comparable between **2a** (2.17 (3) Å) and **1** (2.20 (1) Å), suggesting the stronger Pt–olefin bond strength in **2** than in **1**. Consistent with this is the observation of the much less labile nature of the Pt–olefin bond in **2** as compared with that of **1** (see before).

^{1}H NOE Spectra of $Pt(\eta^3\text{-}CH_2CMeCH_2)(CH_2{=}CHC_6H_5)(C_6F_5)$ (2a). The ^{1}H NMR spectrum of **2a** at 25 °C (Figure 3a) showed the presence of two isomeric forms (**2a**-maj and **2a**-min; relative ratio 2.7/1). All of the styrene and methallyl proton resonances could unambiguously be assigned as shown in Table I (for proton-numbering scheme, see **3** and **4**; $H^{1'} \sim H^{7'}$ for the minor isomer) on

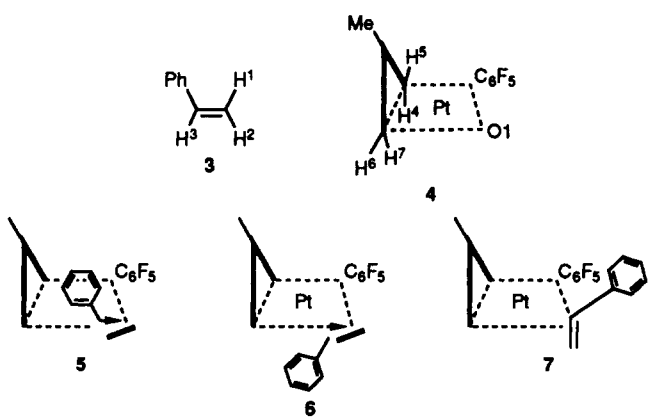

the basis of the following criteria: (1) The NOE experiments described later identify a pair of allylic anti and syn protons (H^4 and H^5, H^7 and H^6) attached to the same carbon. (2) The anti proton resonates at a higher field than the corresponding syn proton.[1c,f,g] (3) The J_{Pt} values for the allylic protons well reflect the ligand trans influence, which is larger for aryl than olefinic ligands.[6] Thus, for example, $J_{Pt\text{-}H^4}$ (61 Hz) is larger than $J_{Pt\text{-}H^7}$ (40 Hz).

When crystals of **2a** were dissolved in $CDCl_3$ at −60 °C and the solution was immediately subjected to ^{1}H NMR measurements, only a single set of resonances due to **2a**-

(6) Appleton, T. G.; Clark, H. C.; Manzer, L. E. *Coord. Chem. Rev.* **1973**, *10*, 335–422.

Table II. Selected Bond Lengths (Å) and Bond Angles (deg) with Esd's in Parentheses

Pt–C(1)	2.17 (3)	Pt–C(2)	2.23 (2)
Pt–C(11)	2.12 (3)	Pt–C(12)	2.15 (2)
Pt–C(13)	2.10 (3)	Pt–C(21)	2.05 (2)
Pt–CET	2.08	Pt–CAL	1.88
C(1)–C(2)	1.41 (3)	C(2)–C(3)	1.51 (3)
C(3)–C(4)	1.42 (3)	C(3)–C(8)	1.39 (3)
C(4)–C(5)	1.37 (4)	C(5)–C(6)	1.38 (4)
C(6)–C(7)	1.39 (4)	C(7)–C(8)	1.38 (4)
C(11)–C(12)	1.42 (4)	C(12)–C(13)	1.31 (4)
C(12)–C(14)	1.50 (4)		
C(21)–C(22)	1.38 (3)	C(21)–C(26)	1.38 (3)
C(22)–C(23)	1.37 (3)	C(23)–C(24)	1.35 (3)
C(24)–C(25)	1.38 (3)	C(25)–C(26)	1.37 (3)
C(22)–F(22)	1.38 (3)	C(23)–F(23)	1.37 (3)
C(24)–F(24)	1.33 (3)	C(25–F(25)	1.35 (3)
C(26)–F(26)	1.36 (3)		
C(1)–Pt–C(2)	37.4 (8)	C(1)–Pt–C(21)	82.3 (8)
C(2)–Pt–C(13)	85.3 (9)	C(11)–Pt–C(13)	65.8 (10)
C(11)–Pt–C(21)	90.3 (8)	CET–Pt–CAL	134.8
CET–Pt–C(21)	101.0	CAL–Pt–C(21)	124.1
Pt–C(1)–C(2)	73.6 (12)	Pt–C(2)–C(1)	69.0 (12)
Pt–C(2)–C(3)	108.1 (12)	C(1)–C(2)–C(3)	122.8 (17)
C(2)–C(3)–C(4)	123.3 (16)	C(2)–C(3)–C(8)	118.6 (16)
C(4)–C(3)–C(8)	118.1 (17)		
Pt–C(11)–C(12)	71.8 (13)	Pt–C(13)–C(12)	74.1 (15)
C(11)–C(12)–C(13)	114.7 (21)	C(11)–C(12)–C(14)	121.2 (20)
C(13)–C(12)–C(14)	122.4 (22)		
Pt–C(21)–C(22)	123.5 (13)	Pt–C(21)–C(26)	122.3 (13)
C(22)–C(21)–C(26)	113.7 (16)		

Figure 3. 400-MHz ^{1}H NMR (a) and NOE difference (b–f) spectra of **2a** in $CDCl_3$ at 25 °C. Selective irradiation was applied at H^3 (b), H^6 (c), $H^{6'}$ (d), H^7 (e), and Ph (f). Overlapping $H^{2'}$, H^5, and $H^{5'}$ resonances could be assigned by NOE difference spectra irradiating at $H^{3'}$, H^4, and $H^{4'}$, respectively. ^{195}Pt satellites are recognized except for $H^{2'}$, H^5, $H^{5'}$, H^6, and $H^{6'}$. W denotes H_2O.

maj was detected. On raising of the temperature, gradual isomerization of **2a**-maj to **2a**-min was observed, and an equilibrium mixture was obtained in ca. 8 h at 0 °C and within 3 min at 25 °C. The following NOE experiments strongly indicate that **2a**-maj assumes a configuration **5** which is similar to that determined by the X-ray diffraction.

The phase-sensitive NOESY spectrum of **2a** shown in Figure 2 revealed positive cross peaks associated with not only pairs of nearby protons contained in the same ligand framework (H^1/H^2, H^1/Ph, H^2/H^3, H^3/Ph, H^4/H^5, H^4/H^7, H^6/H^7, Me/H^5, and Me/H^6 as well as the corresponding proton pairs for the minor isomer) but also a pair of protons each of which belongs to a different ligand (H^3/H^6). Thus, a relatively short distance between H^3 and H^6 is suggested from Figure 2. Since a possible cross peak between H^6 and Ph may have overlapped with the peak due to the $H^{1'}$/Ph' pair and some other meaningful, weaker cross peaks may have been buried in the noise level, we examined more accurate 1-D NOE difference spectra (Figure 3).

Selective irradiation at H^3 (Figure 3b) resulted in small (3%, 1%) but distinct enhancement of the intensity of H^6 and H^7 resonances, respectively, besides the increase of the nearby proton resonances (Ph, H^2), suggesting relatively short distances between H^3 and H^6 as well as between H^3 and H^7. These distances determined by X-ray structure analysis are 2.6 and 2.4 Å. The irradiation at H^6 (Figure 3c) and H^7 (Figure 3e) consistently enhanced the intensity of H^3 resonance. Of further significance is a relatively short distance between Ph (ortho) and H^6 protons as revealed by the selective irradiation at the Ph protons (Figure 3f). These results clearly indicate that *H^6 is close to both H^3 and Ph of the styrene ligand*, fully consistent with the structure **5**. The diastereoisomer of **5**, namely **6**, is also consistent with the NOE experiments. The distances between Me and Ph protons are far above 3 Å even in **5**, according to the X-ray results, so that irradiation at the Ph protons was not helpful in distinguishing between **5** and **6**. At the moment, however, it seems natural to assume that the diastereomeric identity of the solid-state structure is retained in **2a**-maj, which is detected initially upon dissolution.

We also carried out similar NOE experiments for **2a**-min (e.g. Figure 3d) to find a short distance between $H^{3'}$ and $H^{6'}$. It thus seems unlikely that **2a**-min corresponds to a rotamer of **5** in which the C=C bond in **5** has rotated by 180° about the Pt–olefin bond axis.[7] The other clues to the structure of **2a**-min would be an appearance of a peak, though very weak, due to $H^{6'}$ upon irradiating Ph' protons (Figure 3f) and no NOE enhancement of $H^{2'}$ upon irradiating $H^{6'}$ (Figure 3d), disfavoring **7**, another rotamer of **2a**-maj. Moreover, molecular models suggested nonexistence of any sufficiently high-energy transition state during the rotation from **5** to **7** as to allow the appearance of two separate resonances of **5** and **7** at 25 °C. We now suggest that **2a**-min adopts the structure **6** that corresponds to the diastereomer of **5**.

That the complex **2a**, and possibly its substituted styrene analogues also, adopt a solution structure involving the in-plane C=C bond orientation is in good agreement with the considerably smaller stability of an *o*-methylstyrene complex, Pt(η^3-CH_2CMeCH_2)(CH_2=CHC_6H_4Me-*o*)(C_6F_5) (**2f**), as compared with that of **2a** and *p*-methylstyrene analogue Pt(η^3-CH_2CMeCH_2)(CH_2=CHC_6H_4Me-*p*)(C_6F_5) (**2d**) (see later). The *o*-methyl substituent is located, among the two possible ortho sites of the phenyl ring, approximately at a point on the elongated line of the C=C bond but not at the other ortho position owing to interference with the terminal olefinic hydrogen. Thus, it would experience considerable steric interaction with H^6 only in a geometry analogous to **5** and **6** but not in an upright geometry (e.g. **7** or its diastereomer) where the methyl would be far above the coordination plane. The NOE features for **2f** were essentially similar to those for **2a**. Moreover, irradiation of the *o*-methyl signal caused a small increase (ca. 1%) of the H^6 intensity. If the upright configuration were the stable solution structure, the stability of **2f** would have been comparable to or greater than **2a** and the *p*-methylstyrene analogue, as was demonstrated previously[1b] in the authentic upright olefin complexes such as *trans*-$PtCl_2$(olefin)(py). On the other hand, a similar specific decrease of the stability of the *o*-methylstyrene complex was also found in another class of in-plane olefin-coordinated complexes 1.[1b]

Intra- and Intermolecular Epimerization of 2a. Having established that there exist a pair of diastereoisomers in solution, we examined pathway(s) by which the epimerization from **2a**-maj (**5**) to **2a**-min (**6**) (eq 1) proceeds. At least three paths are conceivable: (1) a bimo-

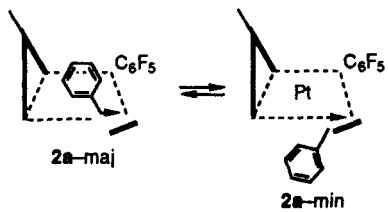

(1)

lecular exchange between coordinated and free styrene, as was most often observed in diastereomeric Pt(II)–olefin complexes;[8] (2) a unimolecular dissociation of free styrene from **2a**, followed by its recoordination using an enantioface opposite to the original one; (3) an intramolecular epimerization without invoking dissociation of the Pt–styrene bond during which the η^3-allyl plane is formally rotated by 180° about the Pt–allyl bond axis.

Path 1 above would indeed contribute to the epimerization in a case in which the free styrene is present in the solution, as is evidenced by independent ligand exchange between styrene of **2a** and a substituted styrene added (see before). If this path is primarily responsible for the epimerization, the rate of epimerization should be increased as the concentration of free styrene is increased.

We examined the epimerization rate both in the absence and the presence of free styrene. To our surprise, we found that the rate of spontaneous isomerization from **2a**-maj to **2a**-min (0.38 h^{-1} in $CDCl_3$ at 0 °C; initial concentration of **2a** is 0.045 M) was not affected by adding free styrene (0.09 M), suggesting the rate of free styrene-mediated epimerization, if any, is much slower. If this result showing that the spontaneous epimerization is faster than the associative epimerization is thought to be a consequence of the rate-determining Pt–styrene bond dissociation, then the rate of displacement of styrene of **2a** by a different olefin (ligand exchange) should also be determined by this step; i.e. the ligand-exchange rate would be comparable to that of the spontaneous epimerization (eq 1). We found that this is not the case, as detailed below.

The pseudo-first-order rate constant of substitution of *p*-chlorostyrene for styrene of **2a** to afford **2c** in $CDCl_3$ at

(7) The X-ray analyses revealed that the conformations of styrene in **2a** and Pt(η^3-CH_2CMeCH_2)(styrene)($SnCl_3$)[1c] are related to each other by an approximately 180° rotation about the Pt–olefin bond axis.

(8) (a) Boucher, H.; Bosnich, B. *J. Am. Chem. Soc.* **1977**, *99*, 6253–6261. (b) Konya, K.; Fujita, J.; Kido, H.; Saito, K. *Bull. Chem. Soc. Jpn.* **1972**, *45*, 2161–2165.

Scheme I

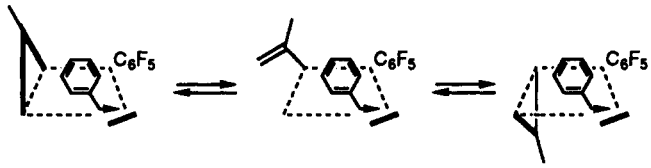

0 °C was 0.07 h^{-1} (initial rate; [**2a**] = 0.05 M, [*p*-chlorostyrene] = 0.5 M; the substitution was too slow to be followed when [*p*-chlorostyrene] = 0.05 M), a value considerably smaller than the spontaneous epimerization rate described above. The substitution rate between **2a** (0.19 M) and *m*-nitrostyrene (0.48 M) to afford **2b** was likewise much slower (half-life ca. 10 min in $CDCl_3$ at 25 °C) than the very rapid isomerization of **2a**-maj to **2a**-min (almost complete within 3 min at 25 °C). From these results, two possibilities, paths 1 and 2 described above, may well be excluded. We suggest that path 3 is primarily responsible for the spontaneous epimerization of **2a**.

The intramolecular epimerization mechanism, namely the formal 180° rotation of the methallyl plane, may be attained either by a real rotation or temporary η^3-allyl to η^1-allyl conversion at the allyl terminal, followed by recoordination of the C=C bond with an enantioface opposite to the original one (see, e.g., Scheme I). Coalescing features of the relevant allyl proton resonances that might be of use for mechanistic considerations were not observed in $CDCl_3$ up to ca. 60 °C. However, upon irradiation of the H^7 signal of the major isomer, a weak but distinct decrease of the intensity of $H^{7'}$ signal occurred (Figure 3e; irradiating $H^{7'}$ consistently decreased the intensity of H^7), even though we could not detect the corresponding, unambiguous negative cross peak in the 2-D NOESY spectra. This spin saturation transfer phenomenon suggests chemical exchange between H^7 and $H^{7'}$ that cannot be ascribed to the real 180° rotation of the η^3-allyl plane because this rotation accompanies the H^7–$H^{4'}$ (and $H^{7'}$–H^4) exchange. Moreover, such rotation was predicted to require considerably high activation barrier in d^8 metal, 16-electron η^3-allyl complexes.[9]

At the moment we propose the transient formation of η^1-allyl species at the allylic end bearing H^4 and H^5 (and $H^{4'}$ and $H^{5'}$) (Scheme I). The epimerization according to Scheme I should give rise to exchange between H^4 and $H^{5'}$ (H^5 and $H^{4'}$ as well) and that between H^7 and $H^{7'}$ (H^6 and $H^{6'}$ as well). The exchange between H^7 and $H^{7'}$ was actually confirmed as shown above. Unfortunately, however, we were unable to test the exchange processes involving H^4, $H^{4'}$, H^5, and $H^{5'}$ by spin transfer saturation method owing to proximity of the resonance due to H^4 and $H^{4'}$ as well as those due to H^5 and $H^{5'}$.

In accord with the formation of a η^1-allyl intermediate at the allylic end trans to styrene (Scheme I), detailed NMR analyses of η^3-allylplatinum complexes indicated[10] that the allylic end located trans to a ligand of weaker trans influence (olefin in the present case) is more likely to be η^1-bonded than the allylic end trans to a stronger ligand. Coordination of the styrene's phenyl group to the vacant site in the intermediate of Scheme I may also assist the η^3-η^1-allyl interconversion. Finally, the following reactivity pattern of **2a** appears of special relevance to the transient formation of the η^1-allylplatinum intermediate. Thus, **2a** decomposed gradually, when heated in $CDCl_3$, affording primarily $CH_2{=}CMe_2$, which is a characteristic product from decomposition of isolable η^1-methallylplatinum complexes in $CDCl_3$.[11]

Table III. Equilibrium Constants (K) of Eq 2 in $CDCl_3$ at 25 °C

Y	K	Y	K
H	1.0	*p*-Me	1.3 ± 0.2
m-NO_2	0.59 ± 0.10	*p*-OMe	1.4 ± 0.2
p-Cl	0.89 ± 0.09	*o*-Me	0.52 ± 0.10

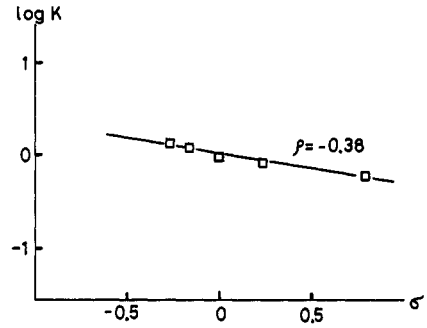

Figure 4. Hammett plot for equilibrium constants (K) of eq 2.

Solution Stability of $Pt(\eta^3\text{-}CH_2CMeCH_2)(CH_2{=}CHC_6H_4Y)(C_6F_5)$. The relative stability of **2a–e**, as expressed by the equilibrium constant of eq 2, was determined by ^1H NMR spectroscopy in the manner analogous to that for **1**. The K value thus determined are summarized in Table III. A Hammett plot for the stability is shown in Figure 4.

$$Pt(\eta^3\text{-}CH_2CMeCH_2)(CH_2{=}CHC_6H_5)(C_6F_5) + CH_2{=}CHC_6H_4Y \overset{K}{\rightleftharpoons} Pt(\eta^3\text{-}CH_2CMeCH_2)(CH_2{=}CHC_6H_4Y)(C_6F_5) + CH_2{=}CHC_6H_5 \quad (2)$$

Of particular note in Table III is that the K values do not deviate much from unity (Hammett $\rho = -0.38$), which is quite different from the trend in **1** ($\rho = -1.32$)[1f] and *trans*-$PtCl_2(CH_2{=}CHC_6H_4Y)py$ (Hammett $\rho^+ = -0.82$),[4] showing the strongly electrophilic nature of the platinum atom to the olefin. Such a novel stability trend as observed in **2** showing very small sensitivity to the electronic effect of the olefin substituent has been found before only in the closely related palladium complexes $Pd(\eta^3\text{-}CH_2CMeCH_2)(CH_2{=}CHC_6H_4Y)(C_6HCl_4\text{-}2,3,5,6)$ ($\rho = -0.25$).[2d] These palladium complexes, however, were characterized only in solutions at low temperature without isolation.

The stability of the *o*-methylstyrene complex **2f** was determined in a similar way, as shown in Table III. As already pointed out before, **2f** was found to be considerably less stable than the unsubstituted and *p*-methyl-substituted styrene complexes, **2a** and **2d**.

Conclusions. The crystal structure determination and ^1H NMR NOE experiments on **2a** indicated preference of the C=C bond lying in the coordination plane both in the solid state and in solution. Preliminary extended Huckel MO calculations on a model, $Pt(\eta^3\text{-}CH_2CHCH_2)(CH_2{=}CH_2)(CH_3)$, indicated[12] that the in-plane C=C geometry is electronically favored over the upright one. This is attributed primarily to the larger π back-bonding in the

(9) Mingos, D. M. P. *Comprehensive Organometallic Chemistry*; Wilkinson, G., Stone, F. G. A., Abel, E. W., Eds.; Pergamon: Oxford, England, 1982; Vol. 3; Chapter 19.
(10) Clark, H. C.; Hampden-Smith, M. J.; Ruegger, H. *Organometallics* **1988**, *7*, 2085–2093.
(11) Numata, S.; Okawara, R.; Kurosawa, H. *Inorg. Chem.* **1977**, *16*, 1737–1741; unpublished results.
(12) Kurosawa, H.; Ikeda, I.; Miki, K.; Kasai, N.; Tatsumi, K.; Nakamura, A. Unpublished results.

in-plane than the upright geometries, since the $d\pi$ orbital of the fragment $Pt(\eta^3\text{-}CH_2CHCH_2)(CH_3)$ suited for π interaction with π^* of the in-plane oriented ethylene lies ca. 0.6 eV higher than that for the π interaction with the upright ethylene.

Comparison of the bond lengths as well as the ligand exchange rate in **2a** with those in **1** clearly demonstrated the stronger Pt–olefin bond strength in the former. These facts are best accommodated by the greater extent of the π-back-bonding interaction between Pt and olefin in **2** than in **1**. The very weak dependency of the stability on the electronic effect of the olefinic substituent in **2** suggests that the π-back-bonding interaction in **2** is in between that in the olefin complexes of very electrophilic metals such as **1** and Zeise's class complexes and that in the nucleophilic, zerovalent complexes of the type $Pt(olefin)(PR_3)_2$.[13] Consistent with this notion, the relevant $d\pi$ orbital of the $Pt(\eta^3\text{-}CH_2CHCH_2)(CH_3)$ fragment lies higher in energy than those in the fragments $[PtCl_3]^-$ (by ca. 0.5 eV) and $[Pt(\eta^3\text{-}CH_2CHCH_2)(PH_3)]^+$ (0.25 eV) but lower than that of the $Pt(PH_3)_2$ fragment (by 0.3 eV).

Experimental Section

Solvents were purified in a standard manner immediately prior to use. Most of the starting materials were obtained from commercial sources. ^1H NMR spectra were obtained on JEOL GSX-400 and Bruker AM-600 spectrometers.

Preparation of 2. Complexes **2b** and **2f** were prepared in a manner similar to that described for **2a**.[2d] Mp of **2b**: 127–130 °C dec. Anal. Calcd for $C_{18}H_{14}NO_2F_5Pt$: C, 38.17; H, 2.49; N, 2.47. Found: C, 38.56; H, 2.57; N, 2.45. Mp of **2f**: 101–102 °C dec. Anal. Calcd for $C_{19}H_{17}F_5Pt$: C, 42.62; H, 3.20. Found: C, 42.80; H, 3.08.

X-ray Structure Determination of 2a. A well-shaped crystal with approximate dimensions of 0.30 × 0.30 × 0.40 mm was mounted on a Rigaku automated, four-circle diffractometer. Crystal data: $C_{18}H_{15}F_5Pt$, fw 521.40, triclinic, space group $P\bar{1}$, a = 6.292 (2) Å, b = 11.874 (4) Å, c = 12.736 (4) Å, α = 117.39 (2)°, β = 82.07 (3)°, γ = 97.50 (4)°, V = 834.3 (5) Å^3, Z = 2, $F(000)$ = 492, D_c = 2.075 g cm^{-3}, μ(Mo Kα) = 8.9 mm^{-1}. Accurate unit cell dimensions were determined by a least-squares fit of 2θ values of 25 reflections. Integrated intensities were collected by the θ–2θ scan technique using graphite-monochromatized Mo Kα radiation (λ = 0.710 69 Å). The scan speed and width were 4° min^{-1} in 2θ and $\Delta 2\theta = (2.0 + 0.70 \tan\theta)°$, respectively. Background intensities were measured for 7.5 s at both ends of a scan. Four standard reflections measured at regular intervals showed no significant decay throughout the data collection. Corrections for Lorentz and polarization effects were applied to the intensity data. No absorption corrections were done in view of the small size and uniform shape of the crystal, which might limit the accuracy of the present structure determination. Totals of 3626 independent reflections were obtained within 2θ up to 54° ($(\sin\theta)/\lambda$ = 0.639 Å^{-1}). The discrepancy factor for symmetry equivalent reflections ($R_{int} = \sum||F| - \langle|F|\rangle|/\sum\langle|F|\rangle$; $\langle|F|\rangle$ = the average value of two or more equivalent reflections) was 0.011.

The structure was solved by the heavy-atom method and refined by the block-diagonal least-squares procedure (HBLS-V),[14] the function minimized being $\sum w(|F_o| - |F_c|)^2$. On the difference Fourier maps after anisotropic refinement, electron densities assigned for all the hydrogen atoms were found at the essentially same positions calculated by stereochemical considerations, which were included in the structure factor calculations. The weighting scheme, $w = (70/|F_o|)^{-2}$ was used for reflections with $|F_o| > 70$, whereas unit weights were employed for those with $|F_o| \le 70$. The final R and R_w values, where $R = \sum||F_o| - |F_c||/\sum|F_o|$ and $R_w = |\sum w(|F_o| - |F_c|)^2/\sum w|F_o|^2\}^{1/2}$, are 0.074 and 0.087 for 3410 observed reflections ($|F_o| > 3\sigma|F_o|$). The atomic scattering factors were taken from ref 15.

(13) Cenini, S.; Ugo, R.; La Monica, G. *J. Chem. Soc. A* **1971**, 409–415.
(14) Ashida, T. *The Universal Crystallographic Computing System-Osaka*, 2nd ed.; The Computation Center: Osaka University, **1979**; p 53.

Table IV. Fractional Atomic Coordinates and Equivalent Isotropic Thermal Parameters (B_{eq}) of Non-Hydrogen Atoms with Esd's in Parentheses

atom	x	y	z	B_{eq}, Å^2
Pt	0.36917 (9)	0.15890 (6)	0.35415 (5)	3.2
C(1)	0.227 (4)	0.3327 (18)	0.3942 (16)	4.7
C(2)	0.293 (3)	0.2772 (16)	0.2717 (15)	3.9
C(3)	0.502 (3)	0.3193 (14)	0.2213 (13)	3.4
C(4)	0.680 (3)	0.3844 (16)	0.2896 (15)	4.0
C(5)	0.863 (4)	0.4218 (18)	0.2386 (19)	5.1
C(6)	0.879 (4)	0.3983 (22)	0.1216 (21)	6.0
C(7)	0.707 (4)	0.3349 (23)	0.0535 (18)	6.0
C(8)	0.522 (3)	0.2960 (18)	0.1029 (15)	4.6
C(11)	0.484 (3)	−0.0089 (18)	0.3388 (19)	5.2
C(12)	0.558 (3)	0.0035 (16)	0.2342 (16)	4.4
C(13)	0.407 (3)	0.0138 (19)	0.1789 (22)	5.6
C(14)	0.792 (4)	0.0346 (22)	0.2074 (22)	6.2
C(21)	0.345 (3)	0.2339 (14)	0.5360 (13)	3.4
C(22)	0.514 (3)	0.3000 (16)	0.6038 (15)	3.7
C(23)	0.506 (3)	0.3417 (17)	0.7236 (16)	4.2
C(24)	0.327 (3)	0.3144 (17)	0.7830 (15)	4.4
C(25)	0.153 (3)	0.2471 (18)	0.7195 (16)	4.5
C(26)	0.166 (3)	0.2074 (15)	0.5996 (14)	3.6
F(22)	0.6991 (16)	0.3337 (12)	0.5500 (10)	5.5
F(23)	0.6792 (20)	0.4079 (13)	0.7852 (11)	6.5
F(24)	0.3162 (22)	0.3508 (14)	0.8992 (10)	6.7
F(25)	−0.0265 (20)	0.2176 (13)	0.7762 (11)	6.6
F(26)	−0.0094 (16)	0.1406 (11)	0.5420 (10)	5.4

The molecular structure is shown in Figure 1.[16] Selected bond lengths and angles are shown in Table II. The final atomic positional parameters, together with the B_{eq} values,[17] are listed in Table IV. Tables of all the bond lengths and angles, anisotropic temperature factors for non-hydrogen atoms, atomic parameters for hydrogen atoms, and observed and calculated structure factors are available as supplementary material (Tables S1–S4).

All the computations were carried out on an ACOS 850 computer at the Crystallographic Research Center, Institute for Protein Research, Osaka University.

Relative Stability Measurement. The other complexes **2c–e** were generated by adding appropriate styrene (0.1–0.05 mmol) to a $CDCl_3$ solution (0.5 mL) of **2a** or **2b** (0.02–0.04 mmol) at 25 °C. The solution was allowed to stand at this temperature for 12 h, and the formation of **2c–e** was confirmed by ^1H NMR spectra. In particular, the following methyl resonances were used for the measurements of the equilibrium concentration of these complexes: **2c**, δ 1.51 (J_{Pt} = 57 Hz, major isomer) and 1.95 (J_{Pt} = 60 Hz, minor isomer; isomer ratio = 2.5/1); **2d**, δ 1.45 (J_{Pt} = 55 Hz, major isomer) and 1.93 (J_{Pt} = 60 Hz, minor isomer; isomer ratio = 2.8/1); **2e**, δ 1.47 (J_{Pt} = 55 Hz, major isomer) and 1.91 (J_{Pt} = 60 Hz, minor isomer; isomer ratio = 2.9/1). For calculation of the equilibrium constant K of eq 2, the combined amount of the two isomers was used as the concentration of each complex, since the isomer ratio did not change greatly from complex to complex.

Rates of Isomerization from 2a-maj to 2a-min and Olefin Ligand Exchange. These rates were all measured by following the change in intensities of the methyl signals by ^1H NMR spectroscopy in $CDCl_3$ at 0 or 25 °C. Samples for the isomerization were prepared by dissolving crystals of **2a** in $CDCl_3$ at −60 °C in an NMR tube. This tube was quickly inserted in an NMR probe precooled at 0 °C. Samples for the ligand exchange were prepared by dissolving crystals of **2a** in $CDCl_3$ in an NMR tube at room temperature, and the tube was kept in a 0 or 25 °C bath for 10 min. Into this solution was injected a known volume of substituted styrene by a syringe, and the tube was quickly placed in a thermostated NMR probe.

(15) *International Tables for X-ray Crystallography*; Kynoch Press: Birmingham, England, 1974; Vol. IV, p 71.
(16) Johnson, C. K. ORTEP-II. Report ORNL-5138; Oak Ridge National Laboratory: Oak Ridge, TN, 1976.
(17) Hamilton, W. C. *Acta Crystallogr.* **1959**, *12*, 609–610.

Acknowledgment. Partial support of this work by Grant-in-aids for Scientific Research from the Ministry of Education, Science, and Culture is gratefully acknowledged.

Supplementary Material Available: Crystallographic information for **2a** including bond lengths and angles (Table S1), anisotropic temperature factors for non-hydrogen atoms (Table S2), and atomic parameters for hydrogen atoms (Table S3) (3 pages); a table of observed and calculated structure factors (Table S4) (9 pages). Ordering information is given on any current masthead page.

Rhodium–Palladium and Rhodium–Platinum Heterobinuclear Complexes Containing the 2-(Diphenylphosphino)pyridine Short-Bite Bridging Ligand. X-ray Crystal Structure of $[(\eta^5\text{-}C_5H_5)(CNBu^t)Rh(\mu\text{-}Ph_2PPy)Pd(CNBu^t)Cl]PF_6$

Sandra Lo Schiavo, Enrico Rotondo, Giuseppe Bruno, and Felice Faraone*

Dipartimento di Chimica Inorganica e Struttura Molecolare, Università di Messina, Salita Sperone 31, Villaggio S. Agata, 98010 Messina, Italy

Received June 19, 1990

Some new RhPd and RhPt heterobinuclear complexes containing the 2-(diphenylphosphino)pyridine (Ph_2PPy) bridging ligand have been prepared by reacting $[Rh(\eta^5\text{-}C_5H_5)(CO)(Ph_2PPy)]$ (**1**) with d^8 palladium(II) and platinum(II) complexes. The reaction of **1** with *cis*-$[Pd(CNBu^t)_2Cl_2]$ gave $[(\eta^5\text{-}C_5H_5)(CNBu^t)Rh(\mu\text{-}Ph_2PPy)Pd(CNBu^t)Cl]Cl$ (**2b**); if the reaction was performed in the presence of $TlPF_6$, the corresponding PF_6^- salt (**2a**) was isolated. The structure of **2a**, containing benzene and methanol molecules of solvation, has been determined by X-ray crystallography. The crystal is monoclinic, with space group $P2_1/n$, and the cell constants are a = 24.485 (3) Å, b = 10.262 (2) Å, c = 17.626 (3) Å, β = 101.40 (4)°, and Z = 4. The structure has been refined to a final R value of 0.045. The cation consists of the $(\eta^5\text{-}C_5H_5)(CNBu^t)Rh$ and $(CNBu^t)ClPd$ moieties held together by the Ph_2PPy bridge and the Rh–Pd bond. The Pd atom exhibits a nearly square-planar coordination geometry, and the ligands about rhodium are disposed in a distorted tetrahedral environment. The angles at rhodium between the centroid of the cyclopentadienyl ring and the other ligands are larger than those formed by the other ligands. The Rh–Pd bond distance is 2.631 (2) Å; the Ph_2PPy is twisted by 35.4 (2)° about the Rh–Pd bond to avoid unfavorable contacts. Compound **2b** readily undergoes metathesis with KI, giving the corresponding iodo derivative $[(\eta^5\text{-}C_5H_5)(CNBu^t)Rh(\mu\text{-}Ph_2PPy)Pd(CNBu^t)I]I$ (**4**); compound **4** was also the product of the reaction of **2b** with CH_3I or CH_2I_2. The reaction of **1** with $[Pd(COD)Cl_2]$ (COD = cycloocta-1,5-diene) occurs by displacement of COD to give $[(C_5H_5)Rh(CO)(\mu\text{-}Ph_2PPy)PdCl_2]$, (**5**). Reaction of **1** with *cis*-$[Pt(DMSO)_2(CH_3)_2]$ (DMSO = dimethyl sulfoxide) gave the compound $[(\eta^5\text{-}C_5H_5)Rh(\mu\text{-}CO)(\mu\text{-}Ph_2PPy)Pt(CH_3)_2]$ (**6**) in which a rhodium–platinum bond is present. The analogous reaction with *cis*-$[Pt(DMSO)_2Cl_2]$ yielded the Rh^{II}–Pt^{I} complex $[(\eta^5\text{-}C_5H_5)RhCl(\mu\text{-}Ph_2PPy)Pt(CO)Cl]$ (**8**); the reaction formally involves the oxidative addition of a d^8 platinum species to a d^8 five-coordinated rhodium(I) complex. The results show that the rigid short-bite Ph_2PPy ligand and the nature of the ligands coordinated to palladium(II) or platinum(II) complexes strongly influence the course of the reactions described.

The synthesis and reactivity of binuclear transition-metal complexes continue to be the subject of considerable interest; this is due to their potential for novel stoichiometric and catalytic reactions.[1-4] In principle, in a heterobimetallic complex each metal center could undergo the reactions observed in their mononuclear compounds; in addition, when the metals are held in close proximity by bridging ligands, novel modes of reactivity, as a consequence of intermediate steps involving formation or breaking of a metal–metal bond, insertion into the metal–metal bond, ligand mobility from terminal to bridging site, and bridging modes involving the substrate molecules, can be observed. Our goal is to prepare homo- and heterobimetallic compounds in which two metal centers are held together by short-bite ligands and to investigate their behavior in small molecule activation processes.

We have recently reported[5,6] the 2-(diphenylphosphino)pyridine (Ph_2PPy) complex $[Rh(\eta^5\text{-}C_5H_5)(CO)(Ph_2PPy)]$, in which the Ph_2PPy acts as a monodentate P-bonded ligand, and its reactions with $[Rh(CO)_2Cl]_2$ and $[Ir(CO)_2(p\text{-toluidine(Cl}]$ to give the unsymmetric complexes $[(\eta^5\text{-}C_5H_5)Rh(\mu\text{-}CO)(\mu\text{-}Ph_2PPy)M(CO)Cl]$ (M = Rh, Ir); interestingly, the complex $[(\eta^5\text{-}C_5H_5)Rh(\mu\text{-}CO)(\mu\text{-}Ph_2PPy)Rh(CO)Cl]$ reacts[6] with alkynes activated by electron-withdrawing groups, giving the tetranuclear species $[(\eta^5\text{-}C_5H_5)Rh(\mu\text{-acetylene})(\mu\text{-}Ph_2PPy)Rh(CO)(\mu\text{-}Cl)]_2$ (acetylene = $CH_3O_2CC_2CO_2CH_3$, $C_2H_5O_2CC_2CO_2C_2H_5$).

The monodentate metal-containing ligand $[Rh(\eta^5\text{-}C_5H_5)(CO)(Ph_2PPy)]$ (**1**) would be suitable for the synthesis of new kinds of heterobimetallic complexes. Here, we report the reactions of **1** with d^8 metal complexes of

(1) *Comprehensive Organometallic Chemistry*; Abel, E. W., Stone, F. G. A., Wilkinson, G., Eds.; Pergamon: Oxford, England, 1982.
(2) Balch, A. L. In *Homogeneous Catalysis with Metal Phosphine Complexes*; Pignolet, L. H., Ed.; Plenum Press: New York, 1983; p 167.
(3) Puddephatt, R. J. *J. Chem. Soc. Rev.* **1983**, 99.
(4) Sanger, A. R. In *Homogeneous Catalysis with Metal Phosphine Complexes*; Pignolet, L. H., Ed.; Plenum Press: New York, 1983; p 216.
(5) Bruno, G.; Lo Schiavo, S.; Rotondo, E.; Arena, C. G.; Faraone, F. *Organometallics* **1989**, *8*, 886.
(6) Rotondo, E.; Lo Schiavo, S.; Bruno, G.; Arena, C. G.; Gobetto, R.; Faraone, F. *Inorg. Chem.* **1989**, *28*, 2944.

0276-7333/91/2310-1613$02.50/0 © 1991 American Chemical Society